Universität Bielefeld

QCD thermodynamics with physical quark masses

York Schröder and Mikko Laine

I. Introduction

The pressure $p(T)$ and its derivatives are central objects in thermodynamics, determining quantities like

- entropy density $s(T) = p'(T)$,
- energy density $e(T) = Ts(T) - p(T)$,
- heat capacity $c(T) = e'(T) = Tp''(T)$.

The main phenomenological applications of the thermodynamic pressure include

- Cosmology:
cooling rate of radiation dominated (flat, $\Lambda = 0$) universe

$$\frac{1}{T}\frac{\mathrm{d}T}{\mathrm{d}t} = -\sqrt{\frac{24\pi e(T)}{m_{\rm Pl}^2}}\frac{s(T)}{c(T)}$$

determines decoupling of various dark matter candidates, fixing their relic densities.

- Heavy ion collisions:
pressure is relevant for hydrodynamic expansion; expansion rate (after thermalization) is (in the ideal limit) given by

$$\partial_\mu T^{\mu\nu} = 0 \quad , \quad T^{\mu\nu} = [p(T) + e(T)]u^\mu u^\nu - p(T)g^{\mu\nu} \; ,$$

with flow velocity $u^\mu(t,x)$.

Theoretically, perturbative QCD corrections to the non-interacting Stefan-Boltzmann law have been determined over the last 30 years, including the relative order $\mathcal{O}(g^6 \ln g)$. The relevant coefficients have been computed as functions of $N_{\rm c}$ and the number of massless quark flavors $N_{\rm f}$ [1], with generalizations to finite quark chemical potentials μ_i [2], and also an extension to weak interactions [3].

A convenient setup for these computations are dimensionally reduced effective field theories, which allow for a transparent organization of contributions from different physical scales. One obtains the general form

$$p_{\rm QCD} = p_{\rm hard} + p_{\rm soft} + p_{\rm ultrasoft} \; ,$$

where the first part contains the contribution of the hard momentum scales ($\sim T$) and hence the LO Stefan-Boltzmann law plus its NLO and further corrections,

$$\frac{p_{\rm hard}}{T^4} = \alpha_{\rm E1}^{\overline{\rm MS}} + g^2\alpha_{\rm E2}^{\overline{\rm MS}} + \mathcal{O}(g^4) \; .$$

The soft and ultrasoft contributions first contribute at relative orders $\mathcal{O}(g^3)$ and $\mathcal{O}(g^6 \ln g)$.

II. Pure-glue pressure to order $\mathcal{O}(g^6)$

The first unknown coefficient in $p_{\rm QCD}$, of order $\mathcal{O}(g^6)$, contains known non-perturbative contributions [4] as well as a yet-unknown perturbative one.

To obtain the best possible description of the pure-glue sector, we attempt to fix the unknown perturbative $\mathcal{O}(g^6)$ coefficient by a phenomenological recipe, using available lattice data at intermediate ($T \sim 3-5T_{\rm c}$) temperatures, see Fig. 1.

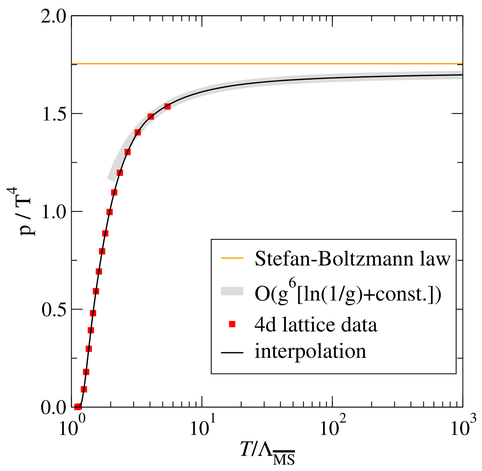

Fig. 1: *A phenomenological interpolating curve for the QCD pressure at $N_{\rm f} = 0$. In the perturbative curve (grey), the $\mathcal{O}(g^6)$ constant has been adjusted to fit lattice data (translated via $T_{\rm c}/\Lambda_{\overline{\rm MS}} \approx 1.20$).*

III. Quark mass thresholds in $p(T)$

Little is known about the quark mass dependence of the QCD pressure. We have analyzed it to NLO [5], using a strategy corresponding to "unquenching":

- Start from $N_{\rm f} = 0$, i.e. $m_q = \infty$
- lower $N_{\rm f}$ quark masses to their physical values
- pressure at any T increases
- estimate "correction factor" describing the increase

This recipe allows for a systematic approach, whose LO result for the "correction factor" is simply the change in the Stefan-Boltzmann law due to quark masses, $\alpha_{\rm E1}^{\overline{\rm MS}}(N_{\rm f})/\alpha_{\rm E1}^{\overline{\rm MS}}(0)$, while the NLO result would be

$$[\alpha_{\rm E1}^{\overline{\rm MS}} + g^2\alpha_{\rm E2}^{\overline{\rm MS}}](N_{\rm f}) \,/\, [\alpha_{\rm E1}^{\overline{\rm MS}} + g^2\alpha_{\rm E2}^{\overline{\rm MS}}](0) \; .$$

We have computed these coefficients (as functions of $T, N_{\rm c}, N_{\rm f}, m_i, \mu_i$), and show the relevant QCD result for $\mu_i = 0$ and physical quark masses in Fig. 2, observing good convergence going from LO to NLO: a 5% effect for $N_{\rm f} = 3$, and even less for the physical case $N_{\rm f} = 4$.

Note that the charm quark contributes already at fairly low temperatures, $T \sim 350\,$MeV.

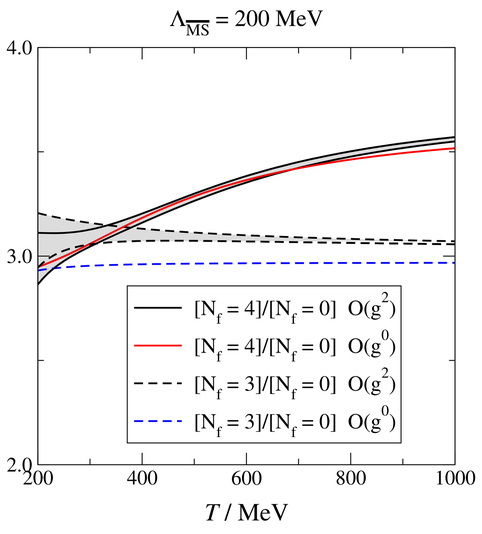

Fig. 2: *The "correction factors" accounting for the effects of quarks, at LO (g^0) and NLO. Grey bands: $\overline{\rm MS}$ scale variations $(0.5...2)\,\bar{\mu}_{opt}$.*

IV. Phenomenological results for QCD

To obtain estimates for thermodynamic quantities including quarks with physical masses, we take the best available $N_{\rm f} = 0$ result (interpolating curve of Fig. 1), and multiply by the "correction factor" (Fig. 2).

To do this, one needs to fix $\Lambda_{\overline{\rm MS}}$ in physical units: We tune it such that our recipe and its first derivative match the pressure produced by the full set of hadronic resonances at a certain T, see Fig. 3. Get $\Lambda_{\overline{\rm MS}}^{\rm (eff)} \approx 175...180\,$MeV as a typical range, depending on $N_{\rm f}$ and experimental errors for m_i.

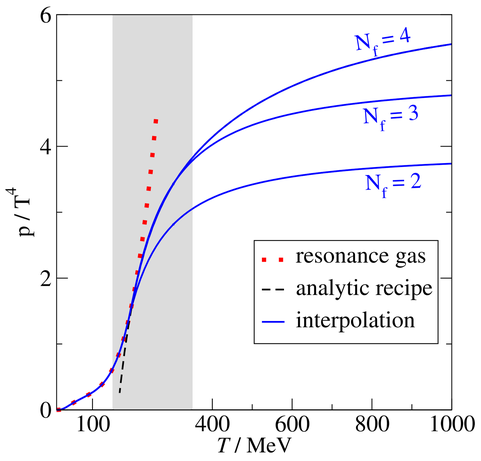

Fig. 3: *Fixing $\Lambda_{\overline{\rm MS}}$ by matching to hadronic resonance gas. Transition region (shaded): lattice simulations needed.*

We are now ready to use our interpolation for other thermodynamic observables, which can be parameterized through effective numbers of bosonic degrees of freedom (Fig. 4, left)

$$g_{\rm eff}(T) \equiv \frac{e(T)}{\left[\frac{\pi^2 T^4}{30}\right]} \; , \quad h_{\rm eff}(T) \equiv \frac{s(T)}{\left[\frac{2\pi^2 T^3}{45}\right]} \; , \quad i_{\rm eff}(T) \equiv \frac{c(T)}{\left[\frac{2\pi^2 T^3}{15}\right]} \; .$$

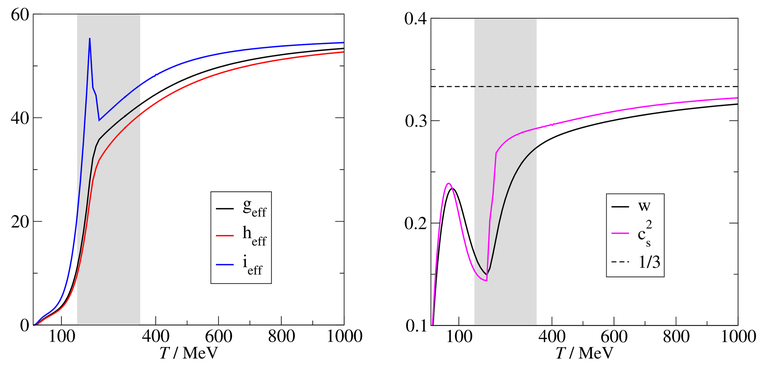

Fig. 4: *Thermodynamic observables, for the physical case $N_{\rm f} = 4$, including the effects of realistic quark masses.*

Other dimensionless ratios are the equation of state and the sound speed (Fig. 4, right panel),

$$w(T) \equiv \frac{p(T)}{e(T)} \quad , \quad c_s^2(T) \equiv \frac{p'(T)}{e'(T)} = \frac{s(T)}{c(T)} \; .$$

The deviation of the equation-of-state $w(T)$ from 1/3 is proportional to the trace anomaly, sometimes also called the interaction measure.

There is a significant amount of structure around the QCD crossover, e.g. a peak in the heat capacity – which is not unexpected in a rapid crossover, since in a 2nd order phase transition it would diverge as $T \to T_{\rm c}$. We also observe a peak in c_s^2 below $T_{\rm c}$ at around 70 MeV, a feature that has not been visible in lattice simulations yet.

Since the phenomenological recipe presented here cannot capture all details of the transition region, an important check would be lattice simulations.

References

[2] For the highest-order coefficient and further references see K. Kajantie *et al.*, Phys. Rev. D 67 (2003) 105008.
[2] A. Vuorinen, Phys. Rev. D 68 (2003) 054017.
[3] A. Gynther and M. Vepsäläinen, JHEP 01 (2006) 060.
[4] F. Di Renzo *et al.*, JHEP 07 (2006) 026.
[5] M. Laine and Y. Schröder, Phys. Rev. D 73 (2006) 085009.